

Design of Unstructured and Protograph-Based LDPC Coded Continuous Phase Modulation

Tarik Benaddi*^{†‡}, Charly Poulliat^{†‡}, Marie-Laure Boucheret ^{†‡}, Benjamin Gadat[§] and Guy Lesthievant*
*CNES-Toulouse [†]University of Toulouse, ENSEEIHT/IRIT
[‡]TéSA - Toulouse [§]Thales Alenia Space-Toulouse

Abstract—In this paper, we derive an asymptotic analysis and optimization of coded CPM systems using both unstructured and protograph-based LDPC codes ensembles. First, we present a simple yet effective approach to design unstructured LDPC codes : by inserting partial interleavers between LDPC and CPM, and allowing degree-1 and degree-2 variable nodes in a controlled pattern, we show that designed codes perform that can operate very close to the maximum achievable rates. Finally, the extension to protograph based codes is discussed. We provide some simple rules to design good protograph codes with good threshold properties.

I. INTRODUCTION

CONTINUOUS phase modulation (CPM) is a class of constant envelope modulation that achieves very good power and bandwidth efficiency. The constant envelope makes this family very powerful when the system contains cheap nonlinear amplifiers or when the communication channel induces non linearities such as satellite communication systems or GSM networks. Due to the complexity of the decoder [1], implementing an optimal detector on embedded receivers restricts the use of CPM to some limited schemes (binary Minimum Shift keying (MSK), binary Gaussian MSK (GMSK)...). Then [2] shows that the CPM modulator can actually be seen as a time-invariant continuous phase encoder (CPE) concatenated with a time-invariant memoryless modulator (MM). Taking advantage of this decomposition and the advent of turbo codes [3], CPM has greatly benefited from the concept of iterative decoding [4]–[7]. Today, CPM regained large attention as a good choice for different stringent wireless communication systems, such as aeronautical communication systems.

Surprisingly, only few works studied concatenated CPM schemes with Low-Density Parity-Check (LDPC) codes. The first related work is due to [8], [9] where density evolution has been used to study of the concatenation of an LDPC code and Minimum Shift Keying (MSK). In [10], a Bit Interleaved Coded-Modulation approach to optimize M-ary CPFSK modulations. Finally, [11]–[13] have considered a non systematic irregular-repeat-accumulate (IRA) like code. The proposed structure replaces the IRA accumulator with a CPM modulator. This has been motivated by the fact that CPM can be seen as a phase accumulator. The proposed scheme finally results in the concatenation of a non systematic Low-Density Generator-Matrix code with CPM. Besides, most of the proposed concatenated systems consider a full interleaver between the LDPC code and the CPM for the asymptotic analysis. Lately, a new class of structured LDPC codes, called protograph codes, has been studied extensively. First

introduced by Thorpe [14], protographs show very good thresholds and low encoder/decoder complexity implementation. In the context of CPM, no study has been made to evaluate the performance and to design protograph-based LDPC codes.

In this paper, we propose an asymptotic analysis to design unstructured LDPC codes for general Rimoldi-based CPM schemes. By introducing partial interleavers, the optimization can be efficiently performed solving a simple linear optimization problem. The second contribution is the asymptotic analysis and design of protograph-based LDPC coded CPMs. The presented design approach can be directly extended to any CPM class, or generally to any trellis coded modulation. In particular, we find out that optimized AWGN [15] protographs do not exhibit necessarily good performance when concatenated with CPM over an additive white Gaussian noise (AWGN) channel.

The paper is structured as follows. In Section II, the system model of the transmitter and the receiver is described. Section III introduces the asymptotic analysis and its inherent assumptions for unstructured LDPC codes. Protograph code analysis and design are derived in Section IV. Finally, simulation results are discussed in Section V.

II. SYSTEM DESCRIPTION

We consider a serially concatenated coded scheme where a binary LDPC encoder is concatenated with a CPM modulator. At the transmitter, a binary message vector $\mathbf{u} \in GF(2)^K$ is first encoded using an LDPC code of rate $R = K/N$ to produce a codeword $\mathbf{c} \in GF(2)^N$. K is the number of information bits, N the codeword length and $GF(2)$ is the binary Galois field. An LDPC code is usually defined using its corresponding binary sparse parity check matrix H of size $M \times N$ with $M = N - K$. \mathbf{c} is a binary vector that belongs to the null space of H if $H\mathbf{c}^T = \mathbf{0}$ where T is the transposition operator. Based on the matrix H , an LDPC code can be represented by its corresponding Tanner graph [16] (see Fig. 2). This later consists in two sets of nodes: the variable nodes (circular vertices) associated with the codeword bits (columns of H) and the check node (square vertices) associated with the parity check constraints (rows of H). An edge joins a variable nodes (VN) n to a check nodes (CN) m if $H(m, n) = 1$. Irregular LDPC codes are usually defined with their edge-perspective degree distribution polynomials $\lambda(x) = \sum_{i=1}^{d_v} \lambda_i x^{i-1}$ and $\rho(x) = \sum_{j=2}^{d_c} \rho_j x^{j-1}$ where λ_i (resp. ρ_j) is the proportion of edges in the Tanner graph connected to variable nodes (VN) of degree i (resp.

to check nodes (CN) of degree j) and d_v (reps. d_c) is maximum VN (resp. CN) degree.

Each code word c is interleaved, Gray-mapped into M -ary symbols $\alpha = \{\alpha_i\}_i$ and finally encoded by the CPM modulator:

$$\begin{aligned} s(t, \alpha) &= \sqrt{\frac{2E_s}{T}} \cos(2\pi f_0 t + \theta(t, \alpha) + \theta_0) \\ &= \Re[s_b(t, \alpha) e^{j2\pi f_0 t}] \end{aligned} \quad (1)$$

with

$$\theta(t, \alpha) = \pi h \sum_{i=0}^{N-1} \alpha_i q(t - iT), \quad q(t) = \begin{cases} \int_0^t g(\tau) d\tau \\ 1/2, t > L \end{cases}$$

f_0 is the carrier frequency, θ_0 the initial phase shift, $\theta(t, \alpha)$ the information carrying phase, $g(t)$ the frequency pulse, $h = k/p$ the modulation index, L the memory and $\Re(\cdot)$ the real part. Practically, the shape of $q(t)$ (rectangular (REC), raised-cosine (RC), ...) and L determine the smoothness of the signal.

At the receiver side, the decoder is formed by the soft input soft output (SISO) CPM detector followed by a SISO LDPC decoder separated by partial interleavers as shown in Fig. 2. It implies a random interleaving of LDPC codewords bits using a different interleaving patterns among variable nodes of the same degree. This is in contrast with approaches that mainly consider full interleaving between the LDPC code and the CPM as classically done for serially concatenated schemes. The rationale behind this design will be made clearer when presenting the asymptotic analysis. The SISO CPM is based on Rimoldi decomposition [2] which splits the CPM modulator into a serial concatenation of the CPE, represented by a trellis, and the MM, seen as a filter bank. The phase of the CPM signal can then be described as:

$$s(t, \alpha) = \sqrt{2E_s/T} \cos(2\pi f_0 t + \psi(t, \alpha) + \psi_0) \quad (2)$$

where the information symbols α are taken in $\{\pm 1, \dots, \pm(M-1)\}$ whatever the parity of M is and figure in the tilted phase as:

$$\begin{aligned} \bar{\psi}(\tau + nT, \alpha) &= \left[2\pi h \sum_{i=0}^{n-L} \alpha_i + 4\pi h \sum_{i=0}^{L-1} \alpha_{n-i} q(\tau + iT) \right. \\ &\quad \left. + W(\tau) \right] \text{ mod } 2\pi, \quad 0 \leq \tau \leq T \end{aligned}$$

where $W(\tau)$ is a data independent term [2].

This decomposition provides a trellis of pM^{L-1} states defined by the tuple $\sigma_n = [U_{n-1}, \dots, U_{n-L+1}, V_n]$ where $V_n = [\sum_{i=0}^{n-L} U_i] \text{ mod } p$, while the MM is formed by pM^L different pulses $\{s_i(t)\}_i$ corresponding to CPE output symbols $X_n = [U_n, \dots, U_{n-L+1}, V_n]$, where U_i is a M -ary modified data digit [2].

The transmitted signal $s(t, \alpha)$ is corrupted with an additive white Gaussian noise (AWGN), having a double-sided power spectral density $N_0/2$. From Eq. (2), the complex baseband representation of the noised signal becomes:

$$y(t) = \sqrt{2E_s/T} \exp\{j\psi(t, \alpha) + n(t)\}, \quad t > 0 \quad (3)$$

The outputs of receiver matched filters bank $\{s^*(T-t)\}$ are sampled once each $(n+1)T$ to obtain the correlator output $\mathbf{y}^n = [y_i^n = \int_{nT}^{(n+1)T} y(l) s_i^*(l) dl]_{1 \leq i \leq pM^L}$.

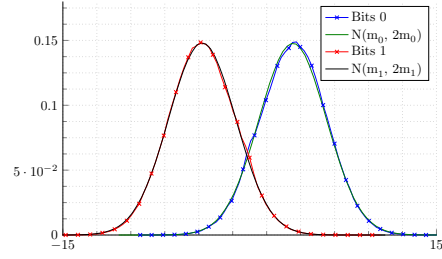


Fig. 1: Probability density function of the LLRs at the output of GSM GMSK decoder vs symmetric Gaussian distribution when a priori mutual information is 0.5. m_0 (resp. m_1) is the expected value of LLRs associated with bits 0 (resp. 1).

It can be shown that $\{\mathbf{y}^n\}_n$ are sufficient statistics to estimate symbols. Furthermore, considering any orthonormal expansion of receiver matched filters bank, the joint probability density function of \mathbf{y}^n can be simplified to $p(\mathbf{y}^n/X_n) \propto \exp\{2\text{Re}(y_i^n)/N_0\}$ [4]. This measure can be used to compute branch metrics of the CPE trellis exploiting the BCJR algorithm [17]. The outer decoder is implemented with the belief propagation (BP) algorithm [18].

In this paper, we assume the following scheduling: a global iteration ℓ is composed of one BCJR forward-backward recursion for the CPM detector followed by one BP iteration (one data-pass plus check-pass update) for the LDPC code. We further assume partial interleavers each one is associated with the VNs set of the same degree. This assumption is in essence equivalent to [20], but it becomes crucial to ensure a practical optimization as it will be shown hereafter.

III. ANALYSIS OF UNSTRUCTURED LDPC CODES

Using density evolution techniques for generalized CPM schemes can be a computationally challenging task, therefore, we mainly consider an EXIT analysis to have insights for the design. First introduced in [19], EXIT chart is a common asymptotic tool that is used to analyze the convergence of iterative systems. The aim of this section is to define the maximum achievable rates that can be obtained with unstructured LDPC codes for CPM. This upper bound will be used later to evaluate the performance of protograph codes. When using EXIT charts, it is commonly assumed that exchanged extrinsic log-likelihood ratio (LLR) can be modelled by consistent and Gaussian-distributed messages. For SISO CPM, Fig. 1 shows that the Gaussian approximation remains acceptable for exchanged messages. Thereby, we can evaluate all messages by only tracking their variance σ^2 or their mean $m = \sigma^2/2$. It is then possible to compute associated mutual information (MI) using a monodimensional function of σ^2 noted $J(\sigma)$ [19]:

$$J(\sigma) = 1 - E_x(\log_2(1 + e^{-x})), \quad x \sim N(\sigma^2/2, \sigma^2)$$

Let $T_{cpm}(\cdot)$ denotes the input-output EXIT transfer characteristic (also referred to as EXIT curve) of the SISO CPM demodulator implicitly depending on the signal to noise ratio E_s/N_0 :

$$I_{cpm, vn} = T_{cpm}(I_{vn, cpm}) \quad (4)$$

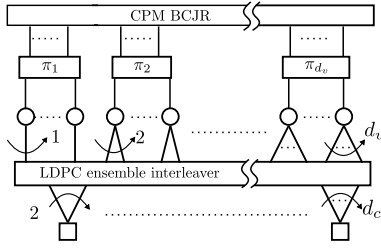


Fig. 2: LDPC code ensemble for joint detection and decoding.

where $I_{cpm,vn}$ (resp. $I_{vn,cpm}$) denotes the a priori (resp. the extrinsic) MI associated with a priori LLR messages at the input (resp. extrinsic LLRs at the output) of the SISO CPM decoder and corresponding bits. Analytic expressions of $T_{cpm}(\cdot)$ are not available, but they can be evaluated by Monte Carlo simulations. In practice, $T_{cpm}(\cdot)$ is approximated by a polynomial curve fitting. Based on the commonly observed generalization of the results of [21] for the binary erasure channel, an upper bound on the maximum achievable code rate, given an E_s/N_0 , for the outer code can be efficiently estimated using the area under the CPM detector EXIT curve, i.e.: $R \leq R^* = \int_0^1 T_{cpm}(I_{vn,cpm}) d(I_{vn,cpm})$.

Under the Gaussian approximation, the combined EXIT function $I_{vn,cn}^\ell$ for the VN and the SISO CPM module for a variable node of degree i at the ℓ^{th} iteration is then given [22] by:

$$I_{vn,cn}^\ell = \sum_{i=1}^{d_v} \lambda_i I_{vn,cn}^\ell(i) \quad (5)$$

with:

$$\begin{cases} I_{vn,cn}^\ell(i) = \\ J \left(\sqrt{(i-1)[J^{-1}(I_{cn,vn}^{\ell-1})]^2 + [J^{-1}(I_{cpm,vn}^\ell(i))]^2} \right) \\ I_{cpm,vn}^\ell(i) = T_{cpm}(J(\sqrt{i}J^{-1}(I_{cn,vn}^{\ell-1}))) \end{cases} \quad (6)$$

where:

- $I_{vn,cn}^\ell(i)$ is the average MI associated with LLR messages passed from a VN of degree i to CNs.
- $I_{cn,vn}^{\ell-1}$ the average MI associated with LLR messages from CNs to VNs.
- $I_{cpm,vn}^\ell(i)$ is the average MI for degree- i VN associated with LLR messages from the CPM decoder to the LDPC decoder. Notice that without the partial interleavers, we are not allowed to write Eq. (6).

Figure 3 plots different VN trajectories as function of node degrees. Notice that VNs EXITs do not start from the origin (0, 0) and that degree-1 VN EXIT corresponds actually to the EXIT transfer function of the SISO CPM decoder. Because it joins the point (1, 1), we are allowed to consider degree-1 VNs as in [8].

For a degree- j CN, the MI $I_{cn,vn}^{\ell-1}$ associated with extrinsic LLRs passed from CN to VN at iteration $\ell-1$ and relative coded bits is known, under reciprocal channel approximation [20], as:

$$I_{cn,vn}^{\ell-1} = 1 - \sum_{j=2}^{d_c} \rho_j J(\sqrt{j-1}J^{-1}(1 - I_{vn,cn}^{\ell-1})) \quad (7)$$

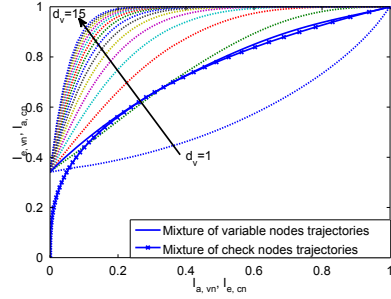


Fig. 3: VN and CN EXIT at $E_s/N_0 = -2dB$.

Threshold at $E_c/N_0 = -2.7dB$			
λ_1	0.1028	ρ_4	0.65
λ_2	0.5506	ρ_5	0.35
λ_9	0.0055		
λ_{10}	0.2917		

TABLE I: Optimized LDPC codes for design rate $R = 0.5$ for binary GMSK

Combining Eqs. (5) and (7) will finally give the recursion Ψ :

$$I_{vn,cn}^\ell = \Psi \left(\lambda(x), \rho(x), T_{cpm}(\cdot), I_{vn,cn}^{\ell-1} \right)$$

Thanks to the partial interleavers, the obtained recursion is a linear function with respect to parameters $\lambda_i, i = 1 \dots d_v$ for a given $\rho(x)$ and a given signal to noise ratio (SNR). With concentrated $\rho(x)$ [22], rate maximization design is equivalent to maximizing the cost function $\sum_i \lambda_i/i$ under:

$$[C0] \text{ Mixture : } \sum_i \lambda_i = 1$$

$$[C1] \text{ Convergence: } \Psi(\lambda(x), \rho(x), T_{cpm}(\cdot), y) > y$$

$$[C2] \text{ Stability: } \lambda_1 < 1 / \left(\sum_{j=2}^{d_c} \rho_j (j-1) T'_{cpm}(1) \right) \quad [23]$$

where $T'_{cpm}(\cdot)$ is the derivative of $T_{cpm}(\cdot)$. This system is efficiently solved by classical linear programming using discretization of the convergence constraint for $y \in [0,1]$. Figure 4 depicts the achievable rates R^* versus the optimized design rates for GSM GMSK ($M=2, L=3, BT=0.3, h=1/2$, Gaussian). One can observe from Table I, that the optimization results in rate-1/2 LDPC profiles that perform asymptotically very close to the achievable rates. Similar curves can be made for the quaternary 2RC and octal 2REC. The corresponding optimized rate-1/2 LDPC profiles are $(\lambda(x) = 0.1232 + 0.6210x + 0.0014x^8 + 0.2545x^9, \rho(x) = 0.8x^2 + 0.2x^3)$ (resp. $(\lambda(x) = 0.2343 + 0.6011x + 0.164x^{10}, \rho(x) = 0.35x + 0.65x^2)$). Associated results are shown in the last section. We point out that we can easily get even more closer to the capacity curve by increasing the maximum variable node degree d_v .

IV. ASYMPTOTIC ANALYSIS OF PROTOGRAPH CODES

Now, we will consider protograph based LDPC codes [14]. Protograph is a small Tanner graph described by a base matrix H where the element $H(q, r)$ is the number of edges between the VN r and the CN q . Unlike LDPC codes, parallel edges are allowed.

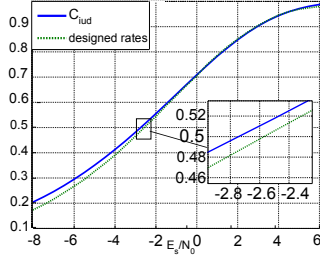


Fig. 4: Achievable and designed rates for GSM GMSK system.

For this class of codes, EXIT charts cannot predict accurately the threshold, i.e. the lowest value of E_s/N_0 that insures reliable decoding assuming infinite code length and a large enough number of turbo iterations. Instead, we use protograph or multidimensional EXIT [24].

For ease of presentation and notation, we use hereafter the following notations relative to the ℓ^{th} iteration:

- $I_{E,v}^{\ell}(q,r)$: extrinsic MI between the code bits associated with VN r and the LLRs sent from this VN to CN q .
- $I_{E,c}^{\ell}(q,r)$: extrinsic MI sent from CN q and the LLRs sent from this CN to VN r .
- $I_{APP}(r)$: a posteriori MI of a VN of degree r .
- $I_{A,cpm}^{\ell}(r)$ and $I_{E,cpm}^{\ell}(r)$: a priori and extrinsic MI at the input (resp. output) BCJR demodulator relative to VN r .

From the VN r (resp. CN q) perspective, $I_{E,c}^{\ell}(q,r)$ (resp. $I_{E,v}^{\ell}(q,r)$) is nothing but the a priori knowledge got from CN q (resp. VN r).

Once the different PEXIT equations have been obtained, we track the evolution of the MI for a given SNR. The threshold is then defined as the lowest value of E_s/N_0 , that insures $I_{APP}(r)$ converges to 1 $\forall r$. For a given size of the protograph, we will use some heuristics inspired from the unstructured LDPC code optimization, to design the general structure of the base matrix. Once a good protograph is chosen, the lifting is done carefully with respect to random circulant permutations coupled with PEG [25] and ACE [26] algorithms.

A. Transfer Function of CPM

As in Section III, the EXIT transfer characteristic of CPM detector seen by the VN r is formally given by:

$$I_{E,cpm}^{\ell}(r) = F(I_{A,cpm}^{\ell-1}(r), E_s/N_0) \quad (8)$$

B. Transfer Function of the Protograph

If $H(q,r) \neq 0$, the VN to CN update equation $\forall(q,r) \in \{1, \dots, M\} \times \{1, \dots, N\}$, is given by:

$$I_{E,v}^{\ell}(q,r) = J \left(\sqrt{\sum_{s \neq i} H(s,r) \left[J^{-1}(I_{E,c}^{\ell-1}(s,r)) \right]^2 + \frac{(H(q,r) - 1) \left[J^{-1}(I_{E,c}^{\ell-1}(q,r)) \right]^2 + \left[J^{-1}(I_{E,cpm}^{\ell}(r)) \right]^2}{(H(q,r) - 1) \left[J^{-1}(I_{E,c}^{\ell-1}(q,r)) \right]^2}} \right) \quad (9)$$

Otherwise, $I_{E,v}^{\ell}(q,r) = 0$.

Using reciprocal channel approximation, CN to VN update is given by:

$$I_{E,c}^{\ell}(q,r) = 1 - J \left(\sqrt{\sum_{s \neq j} H(q,s) \left[J^{-1}(1 - I_{A,c}^{\ell}(q,s)) \right]^2 + \frac{(H(q,r) - 1) \left[J^{-1}(1 - I_{A,c}^{\ell}(q,r)) \right]^2}{(H(q,r) - 1) \left[J^{-1}(1 - I_{A,c}^{\ell}(q,r)) \right]^2}} \right) \quad (10)$$

If $H(q,r) = 0$, then $I_{E,c}^{\ell}(q,r) = 0$.

Seen as an a priori of the SISO CPM component, the MI sent from a VN r to the CPM demodulator is:

$$I_{A,cpm}^{\ell}(r) = J \left(\sqrt{\sum_s H(s,r) \left[J^{-1}(I_{A,v}^{\ell}(s,r)) \right]^2} \right) \quad (11)$$

Combining Eqs. (8), (9), (10) and (11), we can compute the threshold. At the end of each iteration, the a posteriori MI can be evaluated for $r = 1 \dots N$ by:

$$I_{APP}(r) = J \left(\sqrt{\sum_s H(s,r) \left[J^{-1}(I_{A,v}^{\ell}(s,r)) \right]^2 + \frac{(I_{APP}(r) - 1) \left[J^{-1}(I_{A,v}^{\ell}(s,r)) \right]^2}{(I_{APP}(r) - 1) \left[J^{-1}(I_{A,v}^{\ell}(s,r)) \right]^2}} \right) \quad (12)$$

Remark: Equation (12) is different from [27], where the computation of I_{APP} is averaged over all VNs, which actually induces partial interleaver per VN degree.

C. Choice of Protograph Ensemble

Inspired from the analysis of obtained profiles and parity check matrix pattern in Section III, the protograph set is described by a relatively small base matrix that follows a certain pattern and contains small proportion of degree-1, some degree-2 and high-degree VNs. Assuming this, combined with some simple heuristics drawn from our experiments, we observed that good protographs can be found with good encoding properties if we consider base matrices of the following form:

$$H = \begin{pmatrix} x_{1,1} & x_{1,2} & 0 & 0 & 1 & 1 & 0 & 0 \\ x_{2,1} & x_{2,2} & 0 & 1 & 0 & 1 & 1 & 0 \\ x_{3,1} & x_{3,2} & 1 & 0 & 0 & 0 & 1 & 1 \\ x_{4,1} & x_{4,2} & 0 & 0 & 0 & 0 & 0 & 1 \end{pmatrix} \quad (13)$$

In this paper, to limit the size of the protograph ensemble, $x_{q,r}/\forall(q,r) \in \{1, \dots, 4\} \times \{1, 2\}$ are limited to $\{1, 2, 3\}$. Using a computer-based search, some good protographs are found and depicted in Fig. 5.

V. SIMULATION RESULTS

This section gives simulation results for binary LDPC code optimization for GSM GMSK, quaternary 2RC (M=4, gray mapping, L=2, h=1/4, raised cosine) and octal 2REC (M=8, gray mapping, L=2, h=1/4, rectangular) with protograph codes of rate $R = 0.5$. Simulations were performed using around 5000 information bits and 250 turbo iterations. Table II summarizes the achieved thresholds for protographs depicted in Fig. 5. Thresholds of rate-1/2 AR3A and AR4JA from [15] are shown for comparison. We can observe that it is possible to operate at less than 0.3-0.4 dB away from the capacity with an average gain which is 1.5-4 dB better than the AWGN protographs and

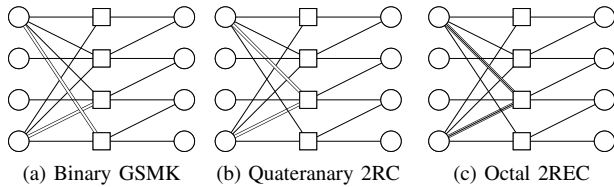


Fig. 5: Optimized protographs for different CPM systems.

	AR3A	AR4JA	CPM protograph	Unstructured LDPC	R^*
binary GSMK	-0.45	-0.20	-2.11	-2.7	-2.76
quaternary 2RC	3.36	3.68	1.36	0.7	0.62
Octal 3RC	7.29	7.92	3.79	2.256	2.25

TABLE II: Optimized asymptotic thresholds E_s/N_0 in dB for protograph-based and unstructured LDPC codes with design rate $R = 0.5$

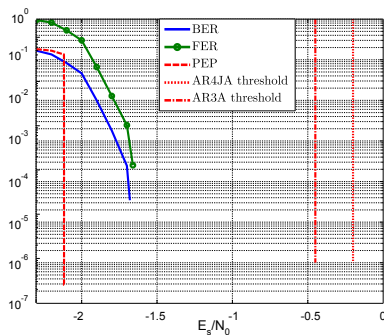


Fig. 6: BER and FER of optimized protographs for GSMK.

a small loss in comparison to the designed unstructured LDPC codes. Figure 6 shows bit error rate (BER), frame error rate (FER) and predicted error probability (PEP) (respectively marked dotted curves, marked dashed curves and marked solid curves) for GSMK. No error floors are observed before 10^{-5} . Asymptotic PEP can be evaluated through described EXIT analysis for a given SNR [15]: after the ℓ^{th} iteration, the expected bit error probability associated with a VN r is related to the a posteriori MI $I_{APP}(r)$ in Eq. (12):

$$P_b(r) = \frac{1}{2} \operatorname{erfc} \left(\frac{J^{-1}(I_{APP}(r))}{2\sqrt{2}} \right) \quad (14)$$

VI. CONCLUSION

We introduced a general framework for the design of unstructured and protograph-based LDPC codes for CPM systems. The discussed method can support any CPM scheme as well as any trellis-based detector. We provided some unstructured LDPC and protograph examples that can achieve good performances. Future investigations will be made to predict error floors region and the best trade off between threshold and error floor performance.

REFERENCES

- [1] John B Anderson, Tor Aulin, and Carl-Erik Sundberg, *Digital phase modulation*, Springer, 1986.
- [2] Bixio E Rimoldi, "A decomposition approach to cpm," *IEEE trans. Inf. Theory*, vol. 34, no. 2, pp. 260–270, 1988.
- [3] Claude Berrou and Alain Glavieux, "Near optimum error correcting coding and decoding: Turbo-codes," *IEEE Trans. Commun.*, vol. 44, no. 10, pp. 1261–1271, 1996.

- [4] Par Moqvist and Tor M Aulin, "Serially concatenated continuous phase modulation with iterative decoding," *IEEE Trans. Commun.*, vol. 49, no. 11, pp. 1901–1915, 2001.
- [5] Alexandre Graell i Amat, Charbel Abdel Nour, and Catherine Douillard, "Serially concatenated continuous phase modulation for satellite communications," *IEEE Trans. Wireless Commun.*, vol. 8, no. 6, pp. 3260–3269, 2009.
- [6] Krishna R Narayanan and Gordon L Stuber, "A serial concatenation approach to iterative demodulation and decoding," *IEEE Trans. Commun.*, vol. 47, no. 7, pp. 956–961, 1999.
- [7] R Chaggara, ML Boucheret, C Bazile, E Bouisson, A Ducasse, and JD Gayraud, "Continuous phase modulation for future satellite communication systems in ka band," in *Information and Communication Technologies: From Theory to Applications, 2004. International Conference on Proceedings. 2004.* IEEE, 2004, pp. 269–270.
- [8] Krishna R Narayanan, Ibrahim Altunbas, and R Sekhar Narayanaswami, "Design of serial concatenated msk schemes based on density evolution," *IEEE Trans. Commun.*, vol. 51, no. 8, pp. 1283–1295, 2003.
- [9] KR Narayanan, I Altunbas, and R Narayanaswami, "On the design of ldpc codes for msk," in *Global Telecommunications Conference, 2001. GLOBECOM'01.* IEEE, 2001, vol. 2, pp. 1011–1015.
- [10] Aravind Ganesan, *Capacity estimation and code design principles for continuous phase modulation (CPM)*, Ph.D. thesis, Texas A&M University, 2003.
- [11] Ming Xiao and Tor Aulin, "Irregular repeat continuous phase modulation," *IEEE Commun. Lett.*, vol. 9, no. 8, pp. 723–725, 2005.
- [12] Shi Cheng, Matthew C Valenti, and Don Torrieri, "Coherent continuous-phase frequency-shift keying: parameter optimization and code design," *IEEE Trans. Wireless Commun.*, vol. 8, no. 4, pp. 1792–1802, 2009.
- [13] Ming Xiao and Tor M Aulin, "On analysis and design of low density generator matrix codes for continuous phase modulation," *IEEE Trans. Wireless Commun.*, vol. 6, no. 9, pp. 3440–3449, 2007.
- [14] J. Thorpe, "Low-density parity-check codes (ldpc) constructed from protographs," *IPN Progress Report*, pp. 42–154, 2003.
- [15] Liva G., *Block Codes Based on Sparse Graphs for Wireless Communication systems*, Ph.D. thesis, University of Bologna, 2006.
- [16] R Tanner, "A recursive approach to low complexity codes," *IEEE trans. Inf. Theory*, vol. 27, no. 5, pp. 533–547, 1981.
- [17] Lalit Bahl, John Cocke, Frederick Jelinek, and Josef Raviv, "Optimal decoding of linear codes for minimizing symbol error rate (corresp.)," *IEEE trans. Inf. Theory*, vol. 20, no. 2, pp. 284–287, 1974.
- [18] Thomas J Richardson and Rüdiger L Urbanke, "The capacity of low-density parity-check codes under message-passing decoding," *IEEE trans. Inf. Theory*, vol. 47, no. 2, pp. 599–618, 2001.
- [19] Stephan Ten Brink, "Convergence behavior of iteratively decoded parallel concatenated codes," *IEEE Trans. Commun.*, vol. 49, no. 10, pp. 1727–1737, 2001.
- [20] Stephan ten Brink, Gerhard Kramer, and Alexei Ashikhmin, "Design of low-density parity-check codes for modulation and detection," *IEEE Trans. Commun.*, vol. 52, no. 4, pp. 670–678, 2004.
- [21] Alexei Ashikhmin, Gerhard Kramer, and Stephan ten Brink, "Extrinsic information transfer functions: model and erasure channel properties," *IEEE trans. Inf. Theory*, vol. 50, no. 11, pp. 2657–2673, 2004.
- [22] Sae-Young Chung, Thomas J Richardson, and Rüdiger L Urbanke, "Analysis of sum-product decoding of low-density parity-check codes using a gaussian approximation," *IEEE trans. Inf. Theory*, vol. 47, no. 2, pp. 657–670, 2001.
- [23] Thomas J Richardson, Mohammad Amin Shokrollahi, and Rüdiger L Urbanke, "Design of capacity-approaching irregular low-density parity-check codes," *IEEE trans. Inf. Theory*, vol. 47, no. 2, pp. 619–637, 2001.
- [24] Gianluigi Liva and Marco Chiani, "Protograph ldpc codes design based on exit analysis," pp. 3250–3254, 2007.
- [25] Xiao-Yu Hu, Evangelos Eleftheriou, and D-M Arnold, "Progressive edge-growth tanner graphs," vol. 2, pp. 995–1001, 2001.
- [26] Sudhanshu John and Hyuck M Kwon, "Approximate cycle extrinsic message degree regular quasi circulant ldpc codes," in *IEEE Military Communications Conference, 2005. MILCOM 2005.* IEEE, 2005, pp. 2877–2881.
- [27] Thuy Van Nguyen, Aria Nosratinia, and Dariush Divsalar, "Protograph-based ldpc codes for partial response channels," in *IEEE International Conference on Communications (ICC), 2012.* IEEE, 2012, pp. 2166–2170.